Puppala PRANEETH [0009-0008-1230-9562]*, *Majety SATHVIKA* [0009-0009-3380-3137]*,
Vivek KOMMAREDDY [0009-0006-8417-7058]*, *Madala SARATH* [0009-0008-1258-3828]*,
Saran MALLELA [0009-0004-4468-6136]*, *K. Suvarna VANI* [0000-0003-1899-9580]*,
Prasun CHKRABART I [0009-0002-9892-7754]**

CLASSIFICATION OF PARKINSON'S DISEASE IN BRAIN MRI IMAGES USING DEEP RESIDUAL CONVOLUTIONAL NEURAL NETWORK (DRCNN)

Abstract

In our aging culture, neurodegenerative disorders like Parkinson's disease (PD) are among the most serious health issues. It is a neurological condition that has social and economic effects on individuals. It happens because the brain's dopamine-producing cells are unable to produce enough of the chemical to support the body's motor functions. The main symptoms of this illness are eyesight, excretion activity, speech, and mobility issues, followed by depression, anxiety, sleep issues, and panic attacks. The main aim of this research is to develop a workable clinical decision-making framework that aids the physician in diagnosing patients with PD influence. In this research, the authors propose a technique to classify Parkinson's disease by MRI brain images. Initially, the input data is normalized using the min-max normalization method, and then noise is removed from the input images using a median filter. The Binary Dragonfly algorithm is then used to select features. In addition, the Dense-UNet technique is used to segment the diseased part from brain MRI images. The disease is then classified as Parkinson's disease or health control using the Deep Residual Convolutional Neural Network (DRCNN) technique along with the Enhanced Whale Optimization Algorithm (EWOA) to achieve better classification accuracy. In this work, the Parkinson's Progression Marker Initiative (PPMI) public dataset for Parkinson's MRI images is used. Indicators of accuracy, sensitivity, specificity and precision are used with manually collected data to evaluate the effectiveness of the proposed methodology.

---

* Velagapudi Ramakrishna Siddhartha Engineering College, Kanuru, Vijayawada, Andhra Pradesh
** ITM SLS Baroda University, Vadodara

1. INTRODUCTION

In recent years, severe diseases have been detected and monitored using a lot of health informatics tools. The monitoring of Parkinson's disease (PD), is typically identified in persons over 60 using artificial learning-based information systems. Parkinson's disease is a central nervous system degenerative condition that primarily damages motor activity in the brain cells. Approximately 7 to 10 million individuals worldwide are affected by this illness, which is one of the most prevalent and rapidly expanding neurodegenerative conditions (Abayomi-Alli et al., 2020; Yaman et al., 2020; Pasha et al., 2020). It is mostly caused by a shortage of dopamine (a neurotransmitter) in the human brain, and it manifests as both motor and non-motor symptoms, including dementia, voice/speech impairment, depression, sluggish thinking, stiffness, bradykinesia, and tremor (Lamba et al., 2022). A neurological condition known as Parkinson's disease is typically found in adults 50 years of age and older. Because the symptoms of Parkinson's disease are typically not captured or avoided until the patient is disturbed, the condition may initially go undetected. It is often characterized by neuronal degeneration in the human brain that results in the nervous system (Kaplan et al., 2022; Senturk et al., 2020). Motor and Non-motor features are the two categories in which the original data obtained from the patients in the features form to classify PD is separated. A patient with Parkinson's disease may exhibit motor characteristics such as tremors, stiffness, and postural instability. While some instances of non-motor aspects are a patient's autonomic, cognitive, and sleep problems (Shu et al., 2020).

The condition of the patient's health is improved by an early diagnosis of PD, which also makes it easier for an experienced practitioner to make quick diagnoses. The traditional techniques used in the early recognition of PD rely exclusively on the information gathered from close examinations and patient interviews. These techniques don't use any kind of sophisticated computing on patient data. Some of the first non-intelligent methods used to diagnose PD were telemonitoring and telediagnosis systems (Mozhdehfarahbakhsh et al., 2021; Griffanti et al., 2020; Chen et al., 2020). Age is the main risk factor. Over 90 genes have been linked to a significant hereditary component of disease risk. Additionally, large populations have shown that some potentially modifiable environmental (such as water pollutants, and pesticides) and other factors (such as coffee, smoking, head trauma, or exercise) have a role in the development of Parkinson's disease (Luo et al., 2022; Prema Arokia Mary et al., 2021).

Parkinson's disease begins with very modest and perhaps undetectable primary causes, but as the disease advances, the signs worsen. Parkinson's disease symptoms differ from person to person. The deseas begins with both non-motor and motor signs. Postural instability (loss of balance), tremors, rigidity, and bradykinesia are examples of motor symptoms. Psychiatric symptoms, dysautonomia, motion sickness, and sensory impairment are examples of non-motor symptoms (autonomic dysfunction). Parkinson's patients frequently experience changes in speech, tremors, sluggish movement (bradykinesia), changes in hand-writing, tight muscles, poor balance and posture, and loss of natural movements (Hossein-Tehrani et al., 2020; Fu et al., 2020; Porter et al., 2020). Ninety percent of Parkinson's patients have vocal dysfunction issues, which is an early sign of the disease, according to research. These vocal abnormalities include hypophonia (reduced volume), monotone (lower pitch), dysphonia (defective voice), and dysarthria (difficulties with articulation).

It might be difficult to make an early diagnosis of Parkinson's for a variety of reasons. Since most patients are over the age of sixty, it takes a lot of time for movement disorder specialists and neurologists to identify this disease after thoroughly analyzing the patient's full medical history and undergoing multiple scans (Zhang et al., 2020). The ability of the doctors to accurately diagnose Parkinson's disease depends on their domain expertise while analyzing the patient's data and symptoms. Unfortunately, there are not enough skilled medical professionals in developing nations like India, Brazil, Argentina, etc. Therefore, identifying or diagnosing Parkinson's is a difficult undertaking because professionals are stressed out by their heavy workload. This inspired the authors to create a decision assistance system that would help doctors diagnose Parkinson's disease. In this paper, a technique to classify Parkinson's disease by MRI brain images is proposed. It has 4 steps to follow. Initially, the input data is normalized using the min-max normalization method, and then noise is removed from the input images using a median filter. The Binary Dragonfly algorithm is then used to select features. In addition, the Dense-UNet technique is used to segment the diseased part from brain MRI images. The disease is then classified as Parkinson's disease or health control using the Deep Residual Convolutional Neural Network (DRCNN) technique along with the Enhanced Whale Optimization Algorithm (EWOA) to achieve better classification accuracy. The key contributions of this paper are,

- In the pre-processing stage, normalizing the input data by using the min-max normalization method and then removing the noise from the input image by utilizing the median filter.
- To feature the selection process, utilizing the Binary Dragonfly Algorithm. Then using the Dense-UNet technique to segment the Parkinson's disease part in brain MRI images.
- Using the deep learning-based classification technique DRCNN to classify the disease if it's Parkinson's disease or normal health control along with Enhanced Whale Optimization Algorithm for better classification accuracy.

This article's remaining sections are organized as follows. Section 2 covers the relevant research on Parkinson's disease classification. Section 3 provides a thorough explanation of the proposed technique and its elements. Section 4 describes the experimental approach. Section 5 reviews the work and makes recommendations for further investigation.

2. LITERATURE REVIEW

In the literature survey, some papers and mentioned all below are reviewed. To detect Parkinson's disease, (Solana-Lavalle et al., 2021) it is recommended that 3D MRI scans be categorized, applied to each gender, and interpreted as follows. This is achievable because the largest dataset currently available was used, with enough observations to segment the dataset by gender. Finding the most pertinent areas of interest for each gender is made possible by the usage of different sets for female and male subjects. (3) The use of multiple classifiers (Bayesian Network, Multi-Layer Perceptron, Naive Bayes, Random Forest, Support Vector Machine, k Nearest Neighbors, Logistic) for a binary decision. (1) The viability of second-order statistics for feature extraction. (2) The use of feature selection techniques to find the most pertinent features while reducing computational complexity. When the regions under study are additionally specified, the binary output from a classifier is of clinical use since doctors must comprehend the rationale for a recommendation by visually inspecting those regions on images.

(Balaji et al., 2020) presented a gait categorization method based on ML that can help the clinician identify the stages of PD. Gait pattern, which is important for evaluating human mobility, is a key biomarker for determining if a person has PD or is in good condition. Therefore, the vertical ground reaction force (VGRF) dataset is used and statistical analysis is used to determine the minimum feature vector. The Shapiro-Wilk test is then used to confirm that the data have a normal distribution, and the correlation-based feature selection technique is then used to identify the salient biomarkers from the temporal and spatial gait pattern features. For kinematic and statistical analyses that predict the severity of PD, four supervised machine learning algorithms Bayes classifier (BC), decision tree (DT), support vector machine (SVM), and ensemble classifier (EC) are utilized.

(Sivaranjini et al., 2020) developed a technique to use deep learning architecture to categorize the MR pictures of PD and HC participants. The public domain database of PPMI is where the photographs needed for classification were found. The MR images are normalized as part of the pre-processing, and the normalized pictures are then subjected to a Gaussian filter. For classification, a convolution neural network known as the AlexNet model is used. To categorize the HC and PD participants, the pre-trained model's weights are used, and the final fully connected layer is refined using the right hyperparameters. The classification results are confirmed once the model has been trained to learn low-level to high-level features.

A DL model was created by (Nagasubramanian et al., 2021) to identify Parkinson's disease. For generating a well-known data pattern, the methodologies utilized in this work are combined with HMM and absolute speech processing algorithms. To improve Parkinson's detection, a single heterogeneous dataset is created from numerous datasets. The approaches ARDNN, ADCNN, and ADNN are suggested for enabling multi-variant acoustic data processing activities based on these technological considerations. The suggested strategy used an appropriate data sampling approach to increase the accuracy rate. More disease-related occurrences were discovered due to the sampling. Results indicate that, in comparison to other existing works, the DMVDA functioned satisfactorily.

Speech problems are one of the earliest indicators of Parkinson's disease and can be used to make a diagnosis. (Caliskan et al., 2017) suggested a Deep Neural Network (DNN) classifier for this purpose which includes stacked auto-encoders and softmax classifiers. To show the power of the deep neural network classifier, several simulations are run over two databases. The proposed classifier's findings are contrasted with those of the most recent classification methodology. The results of the experiment and the statistical analyses demonstrated how effective the deep neural network classifier is in diagnosing Parkinson's disease.

3. PROPOSED METHODOLOGY

Parkinson's disease (PD) is a central nervous system degenerative condition that primarily damages the motor activity in the brain cells. Parkinson's disease begins with very modest and perhaps undetectable primary causes, but as the disease advances, the symptoms worsen. PD symptoms differ from person to person. In this paper, a technique to classify Parkinson's disease by MRI brain images is proposed. It has 4 steps to follow. Initially, the input data is normalized using the min-max normalization method, and then noise is removed

from the input images using a median filter. The Binary Dragonfly algorithm is then used to select features. In addition, the Dense-UNet technique is used to segment the diseased part from brain MRI images. The disease is then classified as Parkinson's disease or health control using the Deep Residual Convolutional Neural Network (DRCNN) technique along with the Enhanced Whale Optimization Algorithm (EWOA) to achieve better classification accuracy.


Fig. 1. Structure of proposed methodology

The framework of the proposed techniques of Parkinson's disease classification is shown in Fig. 1.

3.1. Image Pre-processing

Initially, at the preprocessing stage, the data is normalized, and then the noise from the input images is removed to better predict PD. To standardize the original data and speed up model convergence and increase model correctness, the Min-Max normalization method is chosen and is represented as:

$$x = \frac{x - \min(x)}{\max(x) - \min(x)} \tag{1}$$

The method of normalization involves aligning and encapsulating MRI data to a thorough anatomic template. Because every person's brain differs in size and shape, normalization is necessary to make it easier to compare one brain MRI to another and translate the results into a standard shape and size. Normalization often involves mapping discrete subject-space data to a reference space with a template and a source image. The median filter, which employs a weighted average sum of the surrounding pixels, removes this noise. The median filter does a great job of preserving the edges of an image. After data normalization, images are subjected to a median filter to eliminate noise.

3.2. Feature Selection

After pre-processing the input images, the features of brain MRI data need to be selected. Hence, the Binary Dragonfly Algorithm (BDA) to feature selection is used. The Dragonfly Algorithm (DA), first described by (Mafarja et al., 2018) in 2016, has a discrete variant known as the Binary Dragonfly Algorithm. This algorithm imitates the natural swarming behaviors of dragonflies. The interaction of dragonflies in avoiding the opponent (the worst solution) and locating the food source serves as a model for the exploitative and exploratory mechanisms of DA (the best solution). The position update mechanism in DA uses five primary behaviors: alignment, separation, attraction, cohesion, and distraction.

These actions are each explained as follows:

The goal of separation is to avoid a static collision between the current individual and a nearby individual. The following is how separation is expressed mathematically:

$$S_i = -\sum_{j=1}^{M} X - X_j \tag{2}$$

Where X is a dragonfly's location in a D-dimensional space (the D indicates the number of decision variables), X_j denotes the neighboring individual's location, and M denotes the number of neighbors.

Velocity matching between individuals in a sub-swarm or swarm is made possible through alignment. The calculation for alignment is as follows:

$$A_i = \frac{\sum_{j=1}^{M} V_j}{M} \tag{3}$$

Where M is the total amount of nearby individuals and V_j is their collective velocity.

The term "cohesion" describes the present individual's movement toward the middle of the group of nearby neighbors. The following definition of cohesion:

$$C_i = \frac{\sum_{j=1}^{M} X_j}{M} - X \tag{4}$$

Where M is the total amount of dragonflies in the area, and X_j is the dragonfly's position at the point j^{th}.

In natural swarms, people attract toward food sources and divert predators' attention in addition to alignment, cohesion, and separation. These two principle have also been mathematically modeled in the DA algorithm.

According to attraction, the person should be drawn to potential food sources. The attraction is defined mathematically as:

$$F_i = Xf - X \tag{5}$$

Where Xf denotes where a food source is located.

Distraction means that the person should be kept away from a predator by something external. The following is how the distraction is determined:

$$E_i = Xe + X \tag{6}$$

Where Xe denotes the enemy's location.

These five actions regulate how dragonflies migrate across DA. Each dragonfly's position is updated using the step vector generated as follows:

$$\Delta X_i(t + 1) = (sS_i + \alpha A_i + cC_i + fF_i + eE_i) + w\Delta X_i(t + 1) \tag{7}$$

Where s is the weight of separation, denotes alignment, c denotes cohesion weight, f denotes food weight, w denotes inertia weight, e denotes predator weight, and t denotes the current iteration.

The following equation is used to update the dragonfly positions in the original Digital Atlas:

$$X_i(t + 1) = X_i(t) + \Delta X_i(t + 1) \tag{8}$$

These movements and navigations enable this algorithm to address ongoing issues. In contrast to DA, BDA updates its position vectors using the following equations:

$$X_i^d(t + 1) = \begin{cases} 1 - X_i^d(t) & rand < TF\big(\Delta X_i^d(t + 1)\big) \\ X_i^d(t) & rand < TF\big(\Delta X_i^d(t + 1)\big) \end{cases} \tag{9}$$

$$TF(\Delta X) = \left| \frac{\Delta X}{\sqrt{\Delta X^2 + 1}} \right| \tag{10}$$

where X_i^d is the location of the ith dragonfly in the dth iteration, *rand* displays a number produced at random between 0 and 1, t denotes the current iteration, ΔX is the step vector and $TF(.)$ is the transfer function as illustrated in Equation (9).

The BDA can frequently supply various global and local searches during the optimizations using separation, alignment, and cohesion. The other elements that enable the dragonflies to take advantage of the best options and avoid the bad ones are attraction and distraction. The BDA algorithm is superior due to these five swarming tendencies. The BDA approach is to select the features correctly.

3.3. Segmentation

Once the features were selected, the Dense-UNet technique was used to segment the abnormal part in brain MRI images. Resolution loss occurs as a result of the four down-samplings that U-Net typically does before the concatenate process. Because of the consequent

resolution loss, extensional techniques are needed to increase accuracy. These techniques rely on deep network structures rather than shallow ones. For these reasons, we adopted the dense concatenated U-Net, termed Dense-UNet. The central point behind our proposed Dense-UNet is that it may be created by boosting the information flow across the model. For CXR images, convolution layers yield intermediate feature maps that are very similar to one another. To fully exploit the feature maps' capacity and avoid redundancies, a connection pattern is used, which greatly lowers computing costs. The input of the subsequent layers in Dense-UNet is created by concatenating the outputs of several intermediary layers.

The created feature maps from prior levels are used in all subsequent layers in the planned version of the U-Net, which uses dense connectivity (Fig. 2).
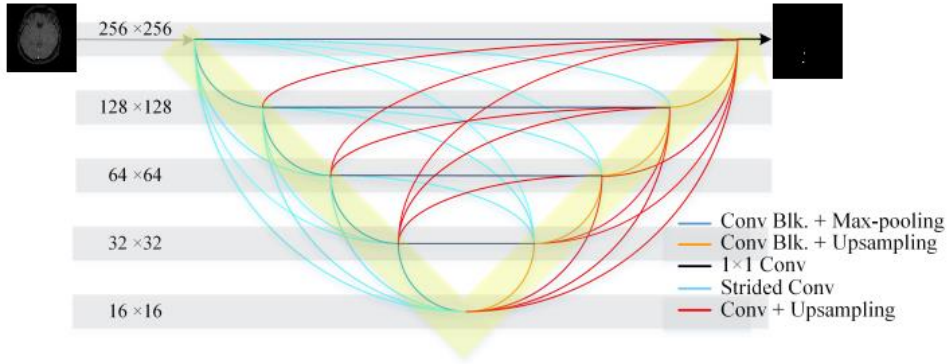

Fig. 2. The proposed Dense-UNet model Architecture

The layers have immediate access to all prior maps during feedforward passes. This adds multi-level properties to the layer, which allows for the integration of various level maps. Additionally, learning is simpler in the backward gradient flow because of deep supervision; gradients can spread throughout all layers, even primary ones (Xin et al., 2019). The loss function's profound impact on the model's many layers makes convergence easier, and information flow allows for a model with lighter construction and much fewer parameters that yet perform well.

The connections in Fig. 2 extract features and balance the size of transferred maps. Between the network's 9 tiers, there are $\frac{9\times(9-1)}{2} = 36$ connections between them. To solve the issue of uneven sizes within distinct layers, stride convolutions, max-pooling, and up-sampling techniques are applied. Equation (11) provides the dimensions of the output feature maps.

$$n_{out} = \left[\frac{n_{in}+2p-k}{s}\right] + 1 \tag{11}$$

Where p displays the padding value around the map, s is the stride step, k is the kernel size, and n_{out} and n_{in} are the sizes of the output and input tensors, respectively. The architecture in Fig. 2 is described in depth as follows:

- Dark blue lines represent the procedures utilized in the Dense-main UNet's body, the max-pooling, and the convolution block (down-sampling by 2). Two convolution layers are the first two parts of a convolution block, which is then followed by a rectified linear activation function and batch normalization.
- The up-sampling and convolution blocks in the expansion path are represented by orange lines. These produce feature maps that are *2n* times as large as the input map.
- The 1x1 Conv connection (in black) simply modifies the depth of feature maps while extracting features; it does not alter the size of the maps. The final segmentation mask is created by transferring feature maps between the output layer and the matching layers.
- Stride convolution layers, represented by the light blue lines, produce smaller-scale feature maps. As seen in Fig. 2, these connections transfer maps to the decoder from the encoder while tuning*s* are used to modify the map sizes.
- The final connection type is represented by the red lines, which include an up-sampling process with scaling factors of 2, 4, and 8.

This Dense-UNet technique segment the diseased part in brain MRI images to better classification of the disease.

3.4. Classification

In the classification stage, the Deep Residual Convolution Neural Network technique is used to classify the disease after segmentation. This deep learning technique works effectively in MRI images. The nonlinear, dynamic, and correlative nature of the variables in complex industrial processes makes it important for latent feature representation to build a DRCNN (Deep Residual Convolutional Neural Network) method (Feng et al., 2021). In contrast to shallow architectures, deep architectures created using the principle of deep learning may reflect complex characteristics and unidentified patterns from countless factors.

The DRCNN network model, which is designed to classify Parkinson's disease, is displayed in Fig. 3. The network model is made up of a lot of blocks, a completely linked layer, and a pooling layer. A unit is a grouping of four connected blocks. Each filter in every unit is a 3x3 filter, which is the most effective. The number of filters in units 1, 2, and 3 are 16, 32, and 64, respectively, to provide multidimensional feature representation as the network becomes deeper. Every convolutional layer, except the first convolutional layer in units 2 and 3, uses stride equal to 1 and zero padding to ensure that output matrices are the same size as input matrices. In units 2 and 3, if the input matrices size is more than 4x4, the stride equals 2 in the first convolutional layer. To integrate the features and provide a little shift invariance, the matrices are reduced by half. The 64 matrices are combined by the average pool layer into a 64-tuples vector, which serves as the network's final feature representation. The 64-tuples vector is changed by the fully connected layer into a vector with the same number of tuples as faults. This vector is used to calculate the loss function. The backpropagation algorithm may determine the gradients of the network using the loss function. The momentum update technique is used to update the network's properties.

Since the DRCNN model is a peer-to-peer deep learning network method, it can make predictions based on the input data directly. The DRCNN classification model is initially developed using a training set. After a significant number of iterations, the DRCNN method can comprehend the complex meaning of the input data and forecast the presence of failure.
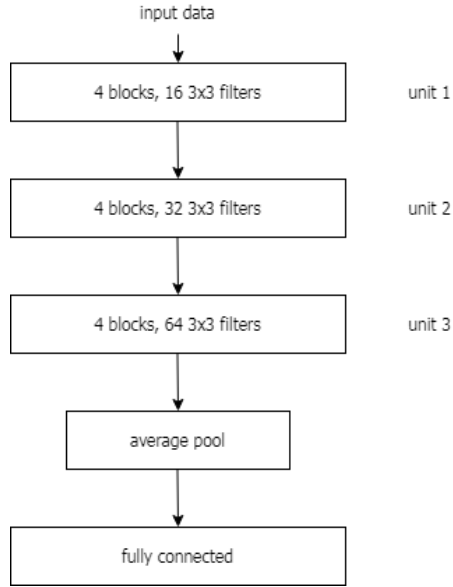
Fig. 3. Classification using the DRCNN model.

After entering the data, this Deep Residual Convolutional Neural Network provides good classification results and accuracy. But we need to improve our proposed methodology performance, so proposed an optimization technique to get better classification accuracy.

3.5. Optimization Algorithm

To classify Parkinson's disease with effective accuracy, the Enhanced Whale Optimization Algorithm (EWOA) is proposed. The WOA was recently added to metaheuristic algorithms by (Chakraborty et al., 2021). The WOA is modeled after the bubble-net hunting approach used to kill humpback whales. They favor hunting small fish or krill schools that are near the surface. To make characteristic bubbles along a circle or "9"-shaped path, humpback whales swim around the prey in a shrinking circle and along a spiral-shaped path at the same time. There is a 50% chance of selecting either the encircling mechanism or the spiral model to update the position of whales during optimization to imitate this behavior in WOA. Their formulas are created in the following way:

1. *Encircling prey that is getting smaller:* In WOA, the best solution at the moment is presumed to be the target prey, and the other search agents attempt to adjust their positions in its direction. The following formula represents this behavior:

$$\vec{X}(t + 1) = \vec{X}^*(t) - A.\vec{D} \tag{12}$$

$$\vec{D} = \left| C.\vec{X}^*(t) - \vec{X}(t) \right| \tag{13}$$

$$A = 2.a.r - a \tag{14}$$

$$C = 2.r \tag{15}$$

134

Where an is progressively decreasing from *2* to *0* for iterations, $\vec{X}$ is a whale location, $\vec{X}^*$ is the historically best position, *t* denotes the current iteration, and r is a random number with uniform distribution in the range (0,1). The absolute value is indicated by the notation "‖".

2. *Spiral bubble-net feeding technique:* To replicate the helix-shaped movement of humpback whales, the following spiral equation is employed between the position of the whale and its prey:

$$\vec{X}(t+1) = e^{bk}.\cos(2\pi k).\vec{D}' + \vec{X}^*(t) \tag{16}$$

$$\vec{D}' = \left|\vec{X}^*(t) - \vec{X}(t)\right| \tag{17}$$

Where *k* is a random number evenly distributed in the range (-1,1) and *b* is a constant used to define the logarithmic spiral's shape.

When *A* < -1 or *A* > 1, the search agent is updated by a random search agent rather than the best search agent to have a global optimizer:

$$\vec{X}(t+1) = \vec{X}_{rand} - A.\vec{D}' \tag{18}$$

$$\vec{D}^" = \left|C.\vec{X}_{rand} - \vec{X}(t)\right| \tag{19}$$

Where $\vec{X}_{rand}$ is chosen at random from the whales in the current iteration.

3.5.1. Enhanced Whale Optimization Algorithm (EWOA)

The WOA is effective in exploring global solutions because its basic premise is clear. A new algorithm known as the EWOA is presented to increase the search reliability, convergence speed, and solution accuracy of WOA. Maintaining the original method's simplicity is important while optimizing an algorithm.

Each iteration extracts a random number between (0, 1) for each whale. Equation (16) is picked if it is more than 0.5; else, Equation (21) is selected to update the position of the whale.

In the EWOA exploration phase, one element of every whale is altered with a random value in the search space with a probability like *p* rather than Equation (18).

$$p = 0.3(1 - iter/iter_{max}) \tag{20}$$

Where $iter_{max}$ and $iter$, respectively, represent the total number of iterations and the current iteration number for the optimization process.

An integer random number between (1, *ng*) is retrieved for each selected whale to determine which design variable should be randomly altered. Next, the interval (0, 1) is used to extract another random number, *q* which is then compared to the probability threshold *p*. According to $x_j = x_{jmin} + random.(x_{jmax} - x_{jmin})$, where a random number evenly distributed in the range (0, 1), the chosen variable x_j is altered if *q<p*.

The improved algorithm ought to be able to maintain a healthy balance between the tendencies toward intensification and diversification. This point and the change mentioned before indicate the definition of Equation (12) as follows:

$$\vec{X}(t+1) = \vec{X}^*(t) - \vec{A}°\vec{D}''' \tag{21}$$

$$\vec{D}' = \vec{r}°\left|\vec{X}(t)\right| \tag{22}$$

$$\vec{A} = 2.\vec{a}°\vec{r} - \vec{a} \tag{23}$$

where $\vec{a}$ is a vector with each component equal to a and $\vec{r}$ is a random vector with each component equally distributed across the (0,1) range. The symbol "°" designates a multiplication of elements one by one. The EWOA algorithm gives better accuracy for Parkinson's disease classification performance.

4. RESULTS AND DISCUSSION

This section compares the approach to "state-of-the-art" techniques by classifying the PD using the dataset's analysis. The following subsections present the results of the evaluation of the methodology based on experimental data.

4.1. Dataset Description

The Parkinson's Progression Marker Initiative (PPMI) dataset's T1 and diffusion-weighted images is employed. In this dataset, 412 individuals with a recent diagnosis of PD and 179 individuals in good health serve as controls. The average age of PD patients is 61, while that of healthy people is 59. Over 93% of the participants are Caucasian, 71% of people with PD are men, and 57% of people with health conditions are men. PPMI dMRI data were collected from 32 different international sites utilizing a consistent technique for Siemens Tim Trio and Siemens Verio 3 Tesla MRI equipment. Using a single b = 0 image and a b-value of 1000 s/mm2, 64 evenly distributed directions were covered by diffusion-weighted images. With a 2 mm isotropic resolution, 116x116 matrix, twofold acceleration, and TR/TE 900/88 ms, a single-shot echo-planar imaging (EPI) sequence was performed. Additionally, a 1 mm3 anatomical T1-weighted MPRAGE picture was captured. Two baseline acquisitions and two additional were performed on each patient a year later. The distribution of patients with right and left onsets is 57% and 43%, respectively. Visit http://www.ppmi-info.org for further details on MRI data collection and processing.

4.2. Quantitative Metrics

The performance of the proposed method for classifying the MRI brain images into PD or Health Control is to give a better result. Here, is given an input brain MRI image from Parkinson's Progression Marker Initiative (PPMI) dataset. Parkinson's disease is a central nervous system degenerative condition that primarily damages motor activity in the brain cells. Parkinson's disease begins with very modest and perhaps undetectable primary causes, but as the disease advances, the symptoms worsen.

Original Picture	After Noise Removal Image	Segmented Images	Classification of Melanoma
			Parkinson's Disease Affected
			Parkinson's Disease Affected
			Normal Health Control
			Parkinson's Disease Affected
			Normal Health Control
			Normal Health Control
			Parkinson's Disease Affected
(a)	(b)	(c)	(d)
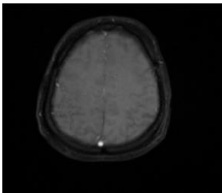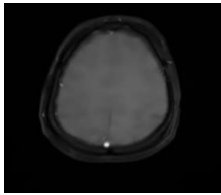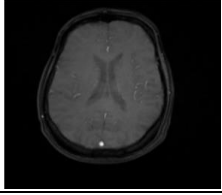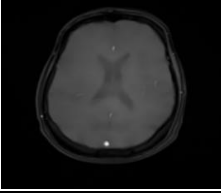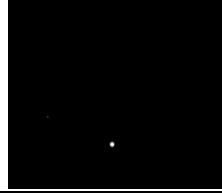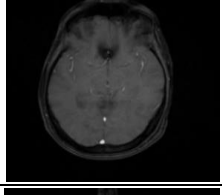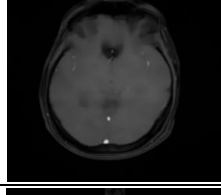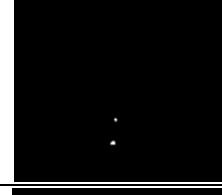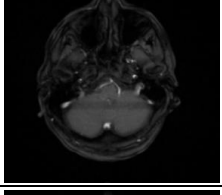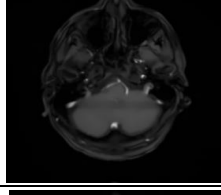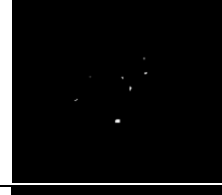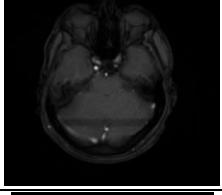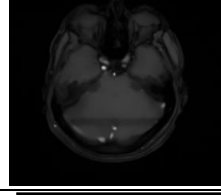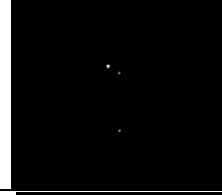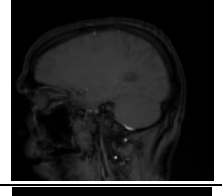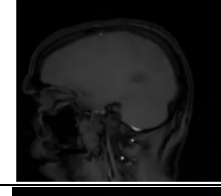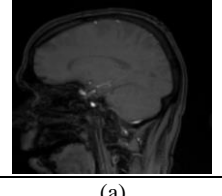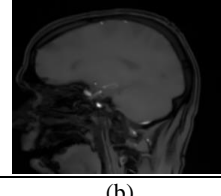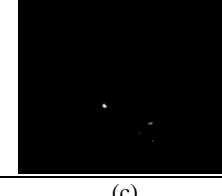
Fig. 4. The experimental outputs: a) Original Image, b) After Noise Removal Image, c) Segmented Images, and d) Classification of Parkinson's disease

This paper proposed a technique to classify Parkinson's disease from MRI brain images. Initially, the input data is normalized using the min-max normalization method, and then noise is removed from the input images using a median filter. The Binary Dragonfly algorithm is then used to select features. In addition, the Dense-UNet technique is used to segment the diseased part from brain MRI images. The disease is then classified as Parkinson's disease or health control using the Deep Residual Convolutional Neural Network (DRCNN) technique along with the Enhanced Whale Optimization Algorithm (EWOA) to achieve better classification accuracy. The findings of the experiment are displayed in Fig. 4 above.

4.3. Evaluation Metrics

As for performance measures, the accuracy, sensitivity, specificity and precision of the proposed method were analyzed. These metrics indicate what follows:

4.3.1. Accuracy

The percentage of samples that were correctly identified relative to all samples is known as accuracy. In general, a classifier performs better the higher accuracy. Equation (24) illustrates the meaning of accuracy.

$$Accuracy = \frac{TP+TN}{TP+FN+FP+TN} \tag{24}$$

4.3.2. Sensitivity

Sensitivity, also known as recall, measures how well a classifier can identify positive samples by representing the percentage of all positive samples that are predicted. Equation (25) defines sensitivity.

$$Sensitivity = \frac{TP}{TP+FN} \tag{25}$$

4.3.3. Specificity

Specificity measures the classifier's capacity to identify negative samples by representing the percentage of all negative samples that are successfully classified. Equation (26) illustrates the definition of specificity.

$$Specificity = \frac{TN}{TN+FP} \tag{26}$$

4.3.4. Precision

Precision is defined as the ratio of precisely anticipated positive occurrences to all anticipated positive observations. Precision is the capacity to do the following things:

$$Precision = \frac{TP}{TP+FP} \tag{27}$$

4.4. Performance Evaluation

In experimental performance, the proposed technique has the highest classification accuracy compared with other existing techniques. Table 1 shows the results for AlexNet (19), DMVDA (20), DNN (21), SVM (18), and the proposed DRCNN on the Parkinson's Progression Marker Initiative (PPMI) dataset in terms of specificity, accuracy, sensitivity, and precision. Based on the results, the proposed methodology has higher classification accuracy values than other existing approaches. So shown are the results of the comparison with and without the optimization algorithm presented as a graph. The proposed approach works well in the authors' database, according to the results. Table 1 shows the findings based on precision, specificity, accuracy, and sensitivity without optimization. Fig. 5 displayed the accuracy analysis of the proposed technique without optimization accuracy compared with other existing techniques. And also Fig. 6 shows the comparison of the proposed technique's classification results with other existing techniques without optimization algorithm graphs for precision, specificity, and sensitivity. The proposed model improved the classification accuracy with less computation time.

Tab. 1. **Using the proposed and compared approaches, calculate Precision, Specificity, Accuracy, and Sensitivity (%) without optimization**

| Approaches	Accuracy (%)	Sensitivity (%)	Specificity (%)	Precision (%)
AlexNet (19)	88.9	90.2	87.84	92.93
DMVDA (20)	93	93.81	89.10	90.76
DNN (21)	87.95	86.21	91.83	89.6
SVM (18)	95.4	92.64	93.12	94.73
Proposed (DRCNN)	97.22	95.93	94.45	96.98
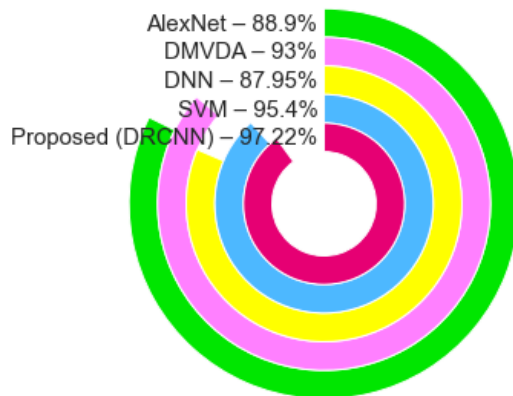
**Fig. 5. Analysis of Accuracy based on different techniques**
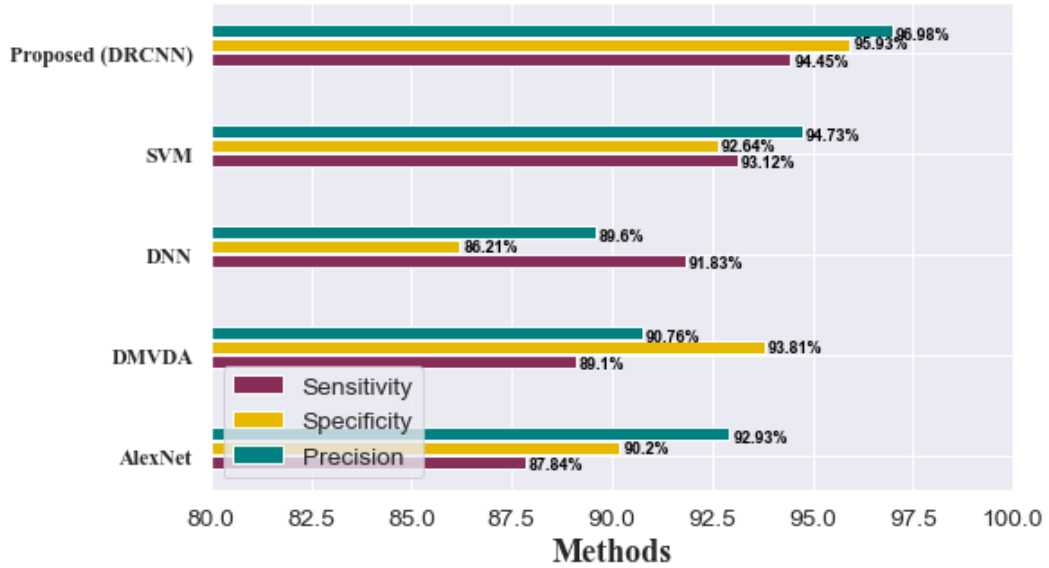
Fig. 6. Comparison of the proposed technique's classification Results with previous Methods without optimization algorithm (a) Sensitivity, (b) Precision, and (c) Specificity

Table 2 shows authors' findings based on precision, specificity, accuracy, and sensitivity with an optimization algorithm. Figure 7 displayed the accuracy analysis of the proposed technique with optimization accuracy compared with other existing techniques. And also Fig. 8 shows the comparison of the proposed technique's classification results with other existing techniques with optimization algorithm graphs for precision, specificity, and sensitivity. Table 2 shows the results for AlexNet (19), DMVDA (20), DNN (21), SVM (18), and the proposed DRCNN with EWOA technique on the Parkinson's Progression Marker Initiative (PPMI) dataset in terms of sensitivity, accuracy, specificity, and precision. Based on the results, we can see that the proposed methodology has higher classification accuracy values than other existing deep learning approaches in terms of recognition rate sensitivity, accuracy, specificity, and precision.

Tab. 2. **Using the proposed and compared approaches, calculate Precision, Specificity, Accuracy, and Sensitivity (%) optimization**

| Approaches	Accuracy (%)	Sensitivity (%)	Specificity (%)	Precision (%)
AlexNet (19)	88.9	90.2	87.84	92.93
DMVDA (20)	93	93.81	89.10	90.76
DNN (21)	87.95	86.21	91.83	89.6
SVM (18)	97.4	92.64	96.12	94.73
Proposed + Optimized (DRCNN)	98.87	96.87	98.13	97.02
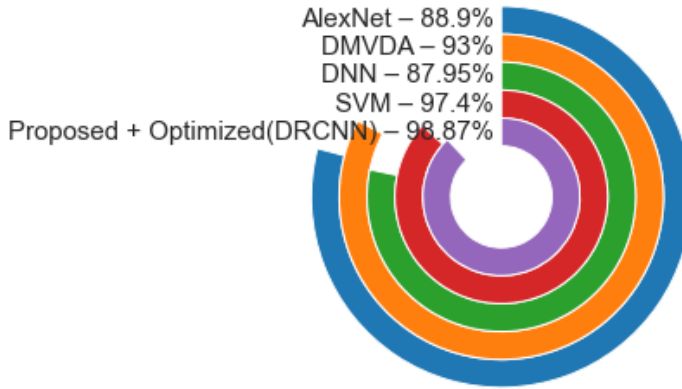
**Fig. 7. Analysis of Accuracy based on different techniques**
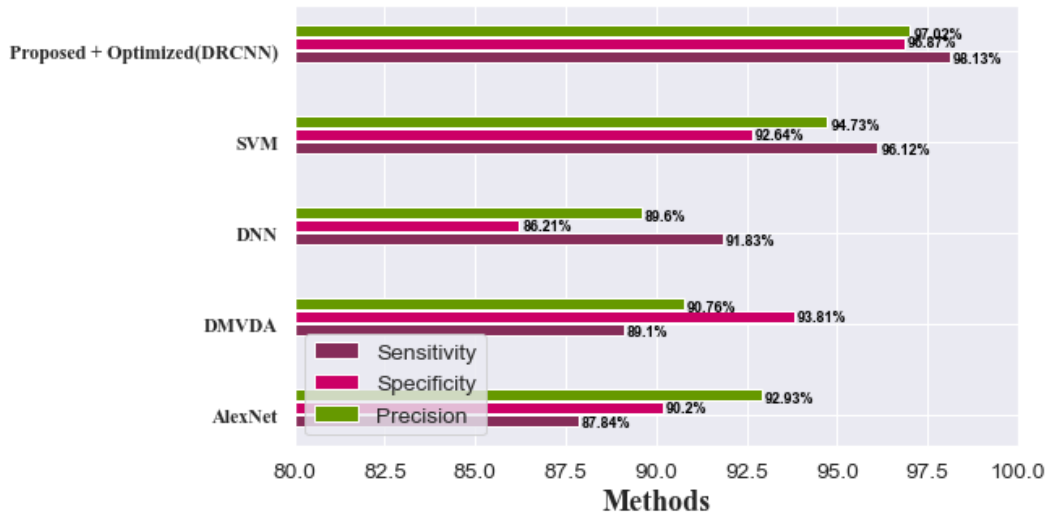
Fig. 8. Comparison of the proposed technique's classification Results with previous Methods with optimization algorithm (a) Sensitivity, (b) Precision, and (c) Specificity

The achieved higher Precision for the proposed technique is 97.02%, compared to 92.93% for AlexNet (19), 90.76% for DMVDA (20), 89.6% for DNN (21), and 94.73% for SVM (18). Additionally, when compared to other existing methodologies, the proposed approach's specificity is superior. DNN (21) has the lowest accuracy rate, at 87.95 percent. The comparison of the proposed method classification results with other methods with optimization algorithm graphs for precision, specificity, and sensitivity is displayed in Fig. 9. Comparing with other existing methods the proposed DRCNN technique achieves higher accuracy with the optimization algorithm. From the experiment analysis, the performance of the classification improved by using the proposed model, and computation time is reduced for training the images.

4.5. Evaluation of training results

After 100 epochs, an accuracy of 97.54% was obtained, which is quite impressive, since the accuracy curves eventually converge. The training and validation accuracy is displayed in Fig. 9.
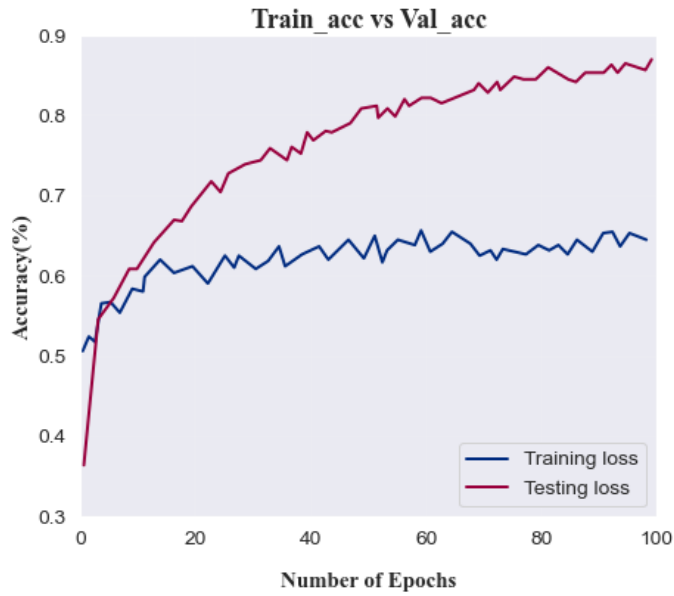
Fig. 9. Training Vs Validation accuracy

The validation Loss curve briefly fluctuates up and down. It proposes that more test results could be advantageous. However, because the variance between Test and Train Loss is minimal and the curve does not increase across epochs, this might be acceptable. The training and validation loss is displayed in Fig. 10.
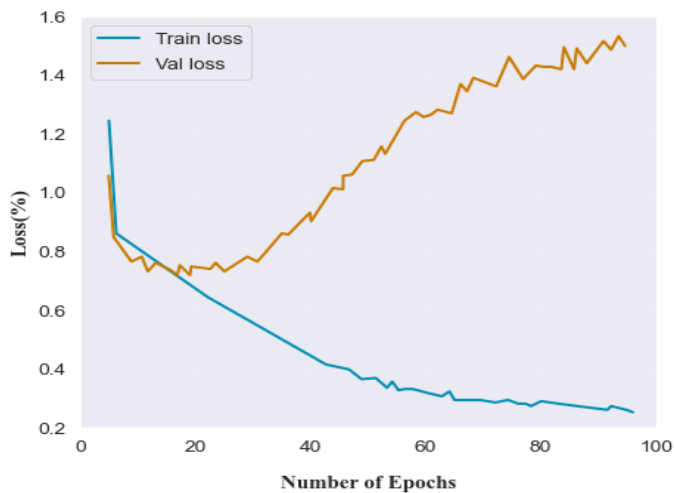
Fig. 10. Training Vs Validation loss

In Figures 9 and 10, the accuracy and loss during training are displayed. Better accuracy and loss estimates are being provided by the DRCNN. Our strategy outperforms previous approaches in the training and validation stages of the Parkinson's disease classification process.

4.6. Computation Time

Another aspect that is discussed is computation time. Deep learning techniques try to make computations less difficult. Comparing the computation times of our proposed DRCNN technique to those of other existing techniques is presented in Table 3. With minimal computing effort, it provides improved classification accuracy. Fig. 11 shows how long it takes to compute using the Parkinson's Progression Marker Initiative (PPMI) dataset using the most recent methodologies and the proposed model.

Tab. 3. Using the proposed and compared approaches, with optimization

| Approaches	Computation Time (ms)
AlexNet (19)	0.17
DMVDA (20)	0.21
DNN (21)	0.25
SVM (18)	0.24
Proposed (DRCNN)	0.15
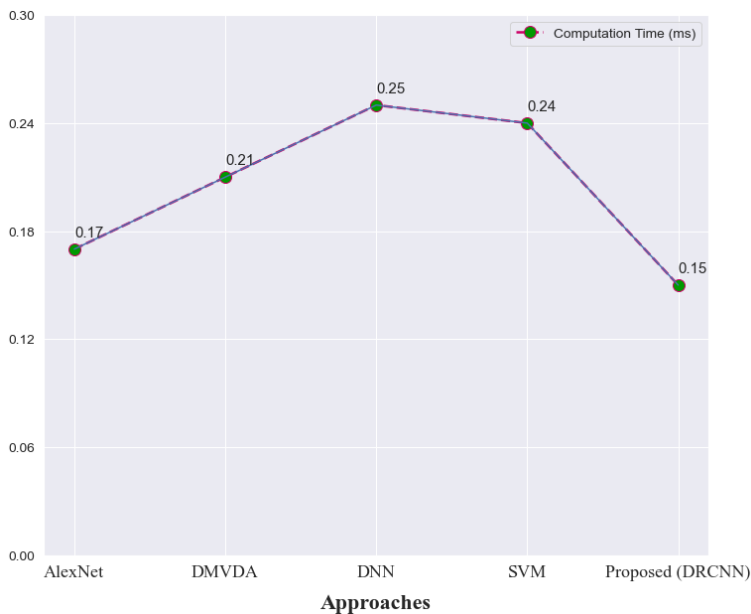
Fig. 11. Comparing the time complexity of the suggested approach to the existing techniques

From Fig. 11, it can be shown that the proposed strategy exceeded computational time more than other techniques.


Fig. 12. Confusion matrix of face objects (a) without optimization, and (b) with optimization

The most used technique for assessing classification errors is the confusion matrix. Based on the provided confusion matrix explanations, developed the confusion matrix for the DRCNN proposed model. The diagram shows that the DRCNN model can classify Parkinson's disease and Normal Health Control appropriately, with the PPMI dataset having the highest ratio of Parkinson's images and the lowest ratio of normal health control images. This shows that the proper categorization of the two statuses has been carried out. The obtained confusion matrix for the cross-validation test of classification is shown in Fig. 12.

5. CONCLUSION

Parkinson's disease begins with very modest and perhaps undetectable primary causes, but the disease signs worsen. Parkinson's disease symptoms differ from person to person. In this paper, a technique to classify Parkinson's disease by MRI brain images is proposed. It has 4 steps to follow. Initially, the input data is normalized using the min-max normalization method, and then noise is removed from the input images using a median filter. The Binary Dragonfly algorithm is then used to select features. In addition, the Dense-UNet technique is used to segment the diseased part from brain MRI images. The disease is then classified as Parkinson's disease or health control using the Deep Residual Convolutional Neural Network (DRCNN) technique along with the Enhanced Whale Optimization Algorithm (EWOA) to achieve better classification accuracy. For these experimental results, Parkinson's MRI image-based Parkinson's Progression Marker Initiative (PPMI) dataset is used. This experiment gives 98.87% classification accuracy using the optimization algorithm. The goal of this paper is to improve the deep learning model to several levels in future research to diagnose Parkinson's disease much more accurately.

Conflict of interests

The authors declare that they have no known competing financial interests or personal relationships that could have appeared to influence the work reported in this paper.

Acknowledgements

Funding

Availability of data and material

Not applicable

Code availability

Not applicable

Authors' contributions

The author confirms sole responsibility for the following: study conception and design, data collection, analysis and interpretation of results, and manuscript preparation.

Ethics approval

This material is the authors' own original work, which has not been previously published elsewhere. The paper reflects the authors' own research and analysis in a truthful and complete manner.

REFERENCE

Abayomi-Alli, O. O., Damaševičius, R., Maskeliūnas, R., & Abayomi-Alli, A. (2020, September). BiLSTM with data augmentation using interpolation methods to improve early detection of parkinson disease. In *2020 15th Conference on Computer Science and Information Systems (FedCSIS)* (pp. 371-380). IEEE. http://doi.org/10.15439/2020F188

Yaman, O., Ertam, F., & Tuncer, T. (2020). Automated Parkinson's disease recognition based on statistical pooling method using acoustic features. Medical Hypotheses, 135, 109483.

Pasha, A., & Latha, P. H. (2020). Bio-inspired dimensionality reduction for Parkinson's disease (PD) classification. Health information science and systems, 8(1), 1-22.

Lamba, R., Gulati, T., Alharbi, H. F., & Jain, A. (2022). A hybrid system for Parkinson's disease diagnosis using machine learning techniques. International Journal of Speech Technology, 25(3), 583-593.

Kaplan, E., Altunisik, E., Firat, Y. E., Barua, P. D., Dogan, S., Baygin, M., & Acharya, U. R. (2022). Novel nested patch-based feature extraction model for automated Parkinson's Disease symptom classification using MRI images. Computer Methods and Programs in Biomedicine, 224, 107030.

Senturk, Z. K. (2020). Early diagnosis of Parkinson's disease using machine learning algorithms. Medical hypotheses, 138, 109603.

Shu, Z., Pang, P., Wu, X., Cui, S., Xu, Y., & Zhang, M. (2020). An integrative nomogram for identifying early-stage Parkinson's disease using non-motor symptoms and white matter-based radiomics biomarkers from whole-brain MRI. Frontiers in aging neuroscience, 12, 457.

Mozhdehfarahbakhsh, A., Chitsazian, S., Chakrabarti, P., Chakrabarti, T., Kateb, B., & Nami, M. (2021). An MRI-based deep learning model to predict Parkinson's disease stages. medRxiv.

Griffanti, L., Klein, J. C., Szewczyk-Krolikowski, K., Menke, R. A., Rolinski, M., Barber, T. R., & Mackay, C. (2020). Cohort profile: the Oxford Parkinson's Disease Centre Discovery Cohort MRI substudy (OPDC-MRI). BMJ open, 10(8), e034110.

Chen, Y., Zhu, G., Liu, D., Liu, Y., Yuan, T., Zhang, X., & Zhang, J. (2020). The morphology of thalamic subnuclei in Parkinson's disease and the effects of machine learning on disease diagnosis and clinical evaluation. Journal of the neurological sciences, 411, 116721.

Luo, J., & Collingwood, J. F. (2022). Effective R2 relaxation rate, derived from dual-contrast fast-spin-echo MRI, enables detection of hemisphere differences in iron level and dopamine function in Parkinson's disease and healthy individuals. Journal of Neuroscience Methods, 382, 109708.

Prema Arokia Mary, G., Suganthi, N., & Hema, M. S. (2021). Early Prediction of Parkinson's disease from Brain MRI Images Using Convolutional Neural Network. Journal of Medical Imaging and Health Informatics, 11(12), 3103-3109.

Hossein-Tehrani, M. R., Ghaedian, T., Hooshmandi, E., Kalhor, L., Foroughi, A. A., & Ostovan, V. R. (2020). Brain TRODAT-SPECT Versus MRI Morphometry in Distinguishing Early Mild Parkinson's disease from Other Extrapyramidal Syndromes. Journal of Neuroimaging, 30(5), 683-689.

Fu, T., Klietz, M., Nösel, P., Wegner, F., Schrader, C., Höglinger, G. U., & Ding, X. Q. (2020). Brain Morphological Alterations Are Detected in Early-Stage Parkinson's disease with MRI Morphometry. Journal of Neuroimaging, 30(6), 786-792.

Porter, E., Roussakis, A. A., Lao-Kaim, N. P., & Piccini, P. (2020). Multimodal dopamine transporter (DAT) imaging and magnetic resonance imaging (MRI) to characterize early Parkinson's disease. Parkinsonism & Related Disorders, 79, 26-33.

Zhang, J., Li, Y., Gao, Y., Hu, J., Huang, B., Rong, S., & Nie, K. (2020). An SBM-based machine learning model for identifying mild cognitive impairment in patients with Parkinson's disease. Journal of the Neurological Sciences, 418, 117077.

Solana-Lavalle, G., & Rosas-Romero, R. (2021). Classification of PPMI MRI scans with voxel-based morphometry and machine learning to assist in the diagnosis of Parkinson's disease. Computer Methods and Programs in Biomedicine, 198, 105793.

Balaji, E., Brindha, D., & Balakrishnan, R. (2020). Supervised machine learning based gait classification system for early detection and stage classification of Parkinson's disease. Applied Soft Computing, 94, 106494.

Sivaranjini, S., & Sujatha, C. M. (2020). Deep learning based diagnosis of Parkinson's disease using convolutional neural network. Multimedia tools and applications, 79(21), 15467-15479.

Nagasubramanian, G., & Sankayya, M. (2021). Multi-variate vocal data analysis for detection of Parkinson disease using deep learning. Neural Computing and Applications, 33(10), 4849-4864.

Caliskan, A., Badem, H., Basturk, A., & YUKSEL, M. (2017). Diagnosis of the parkinson disease by using deep neural network classifier. IU-Journal of Electrical & Electronics Engineering, 17(2), 3311-3318.

Mafarja, M., Aljarah, I., Heidari, A. A., Faris, H., Fournier-Viger, P., Li, X., & Mirjalili, S. (2018). Binary dragonfly optimization for feature selection using time-varying transfer functions. Knowledge-Based Systems, 161, 185-204.

Xin, J., Zhang, X., Zhang, Z., & Fang, W. (2019). Road extraction of high-resolution remote sensing images derived from DenseUNet. Remote Sensing, 11(21), 2499.

Feng, Z., Cai, A., Wang, Y., Li, L., Tong, L., & Yan, B. (2021). Dual residual convolutional neural network (DRCNN) for low-dose CT imaging. Journal of X-Ray Science and Technology, 29(1), 91-109.

Chakraborty, S., Saha, A. K., Sharma, S., Mirjalili, S., & Chakraborty, R. (2021). A novel enhanced whale optimization algorithm for global optimization. Computers & Industrial Engineering, 153, 107086.